

Free-Standing Highly Conductive Transparent Ultrathin Single-Walled Carbon Nanotube Films

Qingfeng Liu,[†] Tsuyohiko Fujigaya,[†] Hui-Ming Cheng,[‡] and Naotoshi Nakashima^{*†§}

Department of Applied Chemistry, Graduate School of Engineering, Kyushu University, 744 Motoooka, Nishi-ku, Fukuoka 819-0395, Japan, Japan Science and Technology Agency (JST), Core Research of Evolutional Science & Technology (CREST), 5 Sanbancho, Chiyoda-ku, Tokyo 102-0075, Japan, and Shenyang National Laboratory for Materials Science, Institute of Metal Research, Chinese Academy of Sciences, Shenyang 110016, P. R. China

Received August 9, 2010; E-mail: nakashima-tcm@mail.cstm.kyushu-u.ac.jp

Abstract: Transparent and conductive single-walled carbon nanotube (SWNT) films are of great importance to a number of applications such as optical and electronic devices. Here, we describe a simple approach for preparing free-standing highly conductive transparent SWNT films with a 20–150 nm thickness by spray coating from surfactant-dispersed aqueous solutions of SWNTs synthesized by an improved floating-catalyst growth method. After the HNO₃ treatment, dipping the SWNT films supporting on glass substrates in water resulted in a quick and nondestructive self-release to form free-standing ultrathin SWNT films on the water surface. The obtained films have sufficiently high transmittance (i.e., 95%), a very low sheet resistance (i.e., ~120 Ω/sq), and a small average surface roughness (i.e., ~3.5 nm for a displayed 10 × 10 μm area). Furthermore, the floating SWNT films on the water surface were easily transferred to any substrates of interest, without intense mechanical and chemical treatments, to preserve their original sizes and network structures. For example, the transferred SWNT films on poly(ethylene terephthalate) films are mechanically flexible, which is a great advantage over conventional indium–tin oxide (ITO) and therefore strongly promise to be “post ITO” for many applications.

Introduction

Two-dimensional random carbon nanotube (CNT) films with unique functionalities can obviate the need for precise control over the spatial position or orientation of individual nanotubes and minimize device-to-device variations even with electronically heterogeneous nanotubes and thus have shown great promise for foreseeable applications especially for thin film devices.^{1–8} It is known that solution-based deposition methods, including dip coating,⁹ spin coating,^{10,11} spray coating,¹² solution casting,¹¹ Langmuir–Blodgett deposition,¹³ and vacuum filtra-

tion,^{14,15} are the most reliable and cost-effective way to fabricate large-area thin films of single-walled carbon nanotubes (SWNTs). For example, Saran et al.⁹ reported a very simple process to fabricate high-quality thin SWNT films via the dip-coating method using laser-ablation SWNTs (a mixture of semiconducting and metallic nanotubes). Recently, we reported the formation of self-organized SWNT composite conducting thin films with honeycomb structures on glass and flexible plastic substrates,^{16,17} which exhibit extremely high electrical conductivity and application to nanoimprint photolithography.¹⁸ However, the solution-based techniques depend on the wettability of the substrates and limit the substrates for applications. Therefore, certain techniques, such as dry transfer, to relocate the SWNT films from the deposited substrates to the target substrates of interest have been established, but the force involved in the transfer process may easily demolish the original network

[†] Kyushu University.

[‡] Chinese Academy of Sciences.

[§] Core Research of Evolutional Science & Technology.

- (1) Star, A.; Tu, E.; Niemann, J.; Gabriel, J. C. P.; Joiner, C. S.; Valcke, C. *Proc. Natl. Acad. Sci. U.S.A.* **2006**, *103*, 921.
- (2) Gruner, G. *J. Mater. Chem.* **2006**, *16*, 3533.
- (3) Fanchini, G.; Miller, S.; Parekh, L. B.; Chhowalla, M. *Nano Lett.* **2008**, *8*, 2176.
- (4) Cao, Q.; Kim, H. S.; Pimparkar, N.; Kulkarni, J. P.; Wang, C. J.; Shim, M.; Roy, K.; Alam, M. A.; Rogers, J. A. *Nature* **2008**, *454*, 495.
- (5) Osuna, R. M.; Hernandez, V.; Navarrete, J. T. L.; Kauppinen, E. I.; Ruiz, V. *J. Phys. Chem. Lett.* **2010**, *1*, 1367.
- (6) Ke, C. H.; Zheng, M.; Zhou, G. W.; Cui, W. L.; Pugno, N.; Miles, R. N. *Small* **2010**, *6*, 438.
- (7) Han, J. T.; Kim, S. Y.; Woo, J. S.; Lee, G. W. *Adv. Mater.* **2008**, *20*, 3724.
- (8) Ci, L. J.; Manikoth, S. M.; Li, X. S.; Vajtai, R.; Ajayan, P. M. *Adv. Mater.* **2007**, *19*, 3300.
- (9) Saran, N.; Parikh, K.; Suh, D. S.; Munoz, E.; Kolla, H.; Manohar, S. K. *J. Am. Chem. Soc.* **2004**, *126*, 4462.
- (10) LeMieux, M. C.; Roberts, M.; Barman, S.; Jin, Y. W.; Kim, J. M.; Bao, Z. N. *Science* **2008**, *321*, 101.

- (11) Meitl, M. A.; Zhou, Y. X.; Gaur, A.; Jeon, S.; Usrey, M. L.; Strano, M. S.; Rogers, J. A. *Nano Lett.* **2004**, *4*, 1643.
- (12) Kaempgen, M.; Duesberg, G. S.; Roth, S. *Appl. Surf. Sci.* **2005**, *252*, 425.
- (13) Li, X. L.; Zhang, L.; Wang, X. R.; Shimoyama, I.; Sun, X. M.; Seo, W. S.; Dai, H. J. *J. Am. Chem. Soc.* **2007**, *129*, 4890.
- (14) Endo, M.; Muramatsu, H.; Hayashi, T.; Kim, Y. A.; Terrones, M.; Dresselhaus, N. S. *Nature* **2005**, *433*, 476.
- (15) Hall, L. J.; Coluci, V. R.; Galvao, D. S.; Kozlov, M. E.; Zhang, M.; Dantas, S. O.; Baughman, R. H. *Science* **2008**, *320*, 504.
- (16) Takamori, H.; Fujigaya, T.; Yamaguchi, Y.; Nakashima, N. *Adv. Mater.* **2007**, *19*, 2535.
- (17) Wakamatsu, N.; Takamori, H.; Fujigaya, T.; Nakashima, N. *Adv. Funct. Mater.* **2009**, *19*, 311.
- (18) Fujigaya, T.; Haraguchi, S.; Fukumaru, T.; Nakashima, N. *Adv. Mater.* **2008**, *20*, 2151.

structure of nanotubes. In this sense, the convenient availability of free-standing thin SWNT films and the safe transfer to other substrates without intense mechanical and chemical treatments are especially important for many applications in their versatility.

Although free-standing SWNT/polymer films have been successfully made from the solution process owing to the extraordinary mechanical flexibility provided by polymers,¹⁹ free-standing ultrathin SWNT films without any polymer coating still remain an unsolved issue. Solid-state spinning is reported only for free-standing multiwalled CNT thick films.^{20–23} Although free-standing thin SWNT films may be directly synthesized,^{24–28} these films thus obtained have a rather loosely packed network structure. A solution-based technique, i.e., postpurification, has been developed to assemble double-walled CNTs into free-standing thin films on a solution surface; however, it presents severe limitations in terms of the film quality (small areas and irregular thickness) and the production efficiency (a process of several days).²⁹ On the other hand, the vacuum filtration technique derived from the ancient art of paper making that involves a long-time and tedious filtration process has been demonstrated as an effective approach for free-standing SWNT films floating on the solution surface when the filtration membranes mechanical-supporting SWNT films were totally dissolved by using wet chemicals.³⁰ However, these wet chemicals not only contaminate the floating SWNT films but also leave chemical wastes behind. Moreover, the size of the SWNT films is limited to the filtration instrument, and therefore, the fabrication process is also not scalable. In addition, when compared to those made by spray coating, especially at a low SWNT loading, the vacuum-filtered ultrathin SWNT films are very notorious for their weak mechanical flexibility and poor conductivities at a high transmittance (i.e., over 90%),³¹ because these ultrathin SWNT films made by vacuum filtration contain partially vertical nanotube alignment trapped in the filter pores by the flow,²¹ which decreases the probability of the SWNTs being connected to each other. Such films possess irregular morphologies and significant roughness, which can lead to short

circuits and overall poor reproducibility during device fabrication.³² Therefore, even for the state-of-the-art solution deposition techniques, it is still difficult to fabricate free-standing ultrathin SWNT films with uniform coverage and high conductivity due to the low solubility and strong intertube interactions of the SWNTs.

We now describe the development of a simple and reliable approach that allows ultrathin SWNT films to be nondestructively self-released into free-standing films on the water surface and easily transferred to the substrates of interest while retaining their original sizes and network structures. High-quality improved floating-catalyst grown SWNTs (F-SWNTs)³³ were used to spray coat uniform thin films from a surfactant-dispersed SWNT aqueous solution. A careful HNO₃-treatment process was introduced to eliminate adhesion of the F-SWNT films to the substrate surface, and then dipping the F-SWNT films supported by glass substrates in water resulted in a nondestructive self-release behavior to form free-standing thin F-SWNT films on the water surface. Such films have a sufficiently high transmittance, very low sheet resistance, and small average surface roughness. In addition, the obtained floating F-SWNT films can also be easily transferred to any substrate, such as flexible polyethylene terephthalate (PET), still maintaining their original sizes and network structures.

Experimental Section

Materials. The F-SWNTs were synthesized by an improved H₂/CH₄-based floating catalyst CVD method.³³ The arc-discharged SWNTs (A-SWNTs) and conventional floating catalyst grown SWNTs (f-SWNTs) were provided by Prof. Y. Ando of Meijo University and Nikkiso Co., Ltd., respectively. The Co–Mo catalytically grown CoMoCAT-SWNTs (CM-SWNTs) and HiPco-SWNTs (H-SWNTs) were purchased from SouthWest Nano Technologies Inc. and Carbon Nanotechnologies Inc., respectively. These SWNTs were used as received. Sodium dodecyl sulfate (SDS) was purchased from Nacalai Tesque Inc.

Preparation of SWNT Films. We started by mixing each type of SWNTs with 1 wt % SDS to make a SWNT dispersion with a concentration of ~0.6 mg/mL. Such suspension was ultrasonically agitated using a probe sonicator (Branson, UD-200) with an output sonication power of <40 W (<~1 W mL⁻¹) for 5–40 min and then sonicated in a bath-type sonicator (Branson, 5510) for 1–10 h, followed by centrifugation (Hitachi, Himac CS 100GXL) for 1–2 h at 19 000g in order to separate out the undissolved SWNT bundles and catalyst impurities. It should be noted that the microstructures of the SWNTs did not change much in the solvation process in our experiments (see Supporting Information, Figure S1).

To make uniform SWNT films with high quality, the upper 70% of the suspension was further diluted 3 times (~0.2 mg/mL) with deionized water. Thin films were directly spray-coated onto the glass substrates by using an airbrush pistol. During the spraying process, the glass substrates were maintained at ~100 °C in order to prevent the formation of fine droplets on the surface of the substrates. When the spray process terminated, the films was immersed into deionized water for 1–2 h to remove the superfluous SDS surfactant and then dried at 90 °C for 1–2 h. Special care for the choice of the SWNT concentration, the nozzle size of the pistol, and the distance from the pistol nozzle to the glass substrates should be simultaneously done in order to obtain uniform ultrathin SWNT films with a high quality.

Finally, the spray-coated SWNT films supported on glass substrates were immersed in a ~5.5 M HNO₃ solution for 1–24 h

- (19) Gu, H.; Swager, T. M. *Adv. Mater.* **2008**, *20*, 4433.
- (20) Xiao, L.; Chen, Z.; Feng, C.; Liu, L.; Bai, Z. Q.; Wang, Y.; Qian, L.; Zhang, Y. Y.; Li, Q. Q.; Jiang, K. L.; Fan, S. S. *Nano Lett.* **2008**, *8*, 4539.
- (21) Zhang, M.; Fang, S. L.; Zakhidov, A. A.; Lee, S. B.; Aliev, A. E.; Williams, C. D.; Atkinson, K. R.; Baughman, R. H. *Science* **2005**, *309*, 1215.
- (22) Liu, K.; Sun, Y. H.; Chen, L.; Feng, C.; Feng, X. F.; Jiang, K. L.; Zhao, Y. G.; Fan, S. S. *Nano Lett.* **2008**, *8*, 700.
- (23) Feng, C.; Liu, K.; Wu, J. S.; Liu, L.; Cheng, J. S.; Zhang, Y. Y.; Sun, Y. H.; Li, Q. Q.; Fan, S. S.; Jiang, K. L. *Adv. Funct. Mater.* **2010**, *20*, 885.
- (24) Ma, W. J.; Song, L.; Yang, R.; Zhang, T. H.; Zhao, Y. C.; Sun, L. F.; Ren, Y.; Liu, D. F.; Liu, L. F.; Shen, J.; Zhang, Z. X.; Xiang, Y. J.; Zhou, W. Y.; Xie, S. S. *Nano Lett.* **2007**, *7*, 2307.
- (25) Liu, Q. F.; Ren, W. C.; Wang, D. W.; Chen, Z. G.; Pei, S. F.; Liu, B. L.; Li, F.; Cong, H. T.; Liu, C.; Cheng, H. M. *ACS Nano* **2009**, *3*, 707.
- (26) Liu, C.; Fan, Y. Y.; Liu, M.; Cong, H. T.; Cheng, H. M.; Dresselhaus, M. S. *Science* **1999**, *286*, 1127.
- (27) Liu, Q. F.; Ren, W. C.; Li, F.; Cong, H. T.; Cheng, H. M. *J. Phys. Chem. C* **2007**, *111*, 5006.
- (28) Pint, C. L.; Xu, Y. Q.; Pasquali, M.; Hauge, R. H. *ACS Nano* **2008**, *2*, 1871.
- (29) Wei, J. Q.; Zhu, H. W.; Li, Y. H.; Chen, B.; Jia, Y.; Wang, K. L.; Wang, Z. C.; Liu, W. J.; Luo, J. B.; Zheng, M. X.; Wu, D. H.; Zhu, Y. Q.; Wei, B. Q. *Adv. Mater.* **2006**, *18*, 1695.
- (30) Wu, Z. C.; Chen, Z. H.; Du, X.; Logan, J. M.; Sippel, J.; Nikolou, M.; Kamaras, K.; Reynolds, J. R.; Tanner, D. B.; Hebard, A. F.; Rinzler, A. G. *Science* **2004**, *305*, 1273.
- (31) Li, Z. R.; Kandel, H. R.; Dervishi, E.; Saini, V.; Xu, Y.; Biris, A. R.; Lupu, D.; Salamo, G. J.; Biris, A. S. *Langmuir* **2008**, *24*, 2655.

- (32) Tenent, R. C.; Barnes, T. M.; Bergeson, J. D.; Ferguson, A. J.; To, B.; Gedvilas, L. M.; Heben, M. J.; Blackburn, J. L. *Adv. Mater.* **2009**, *21*, 3210.
- (33) Liu, Q. F.; Ren, W. C.; Chen, Z. G.; Wang, D. W.; Liu, B. L.; Yu, B.; Li, F.; Cong, H. T.; Cheng, H. M. *ACS Nano* **2008**, *2*, 1722.

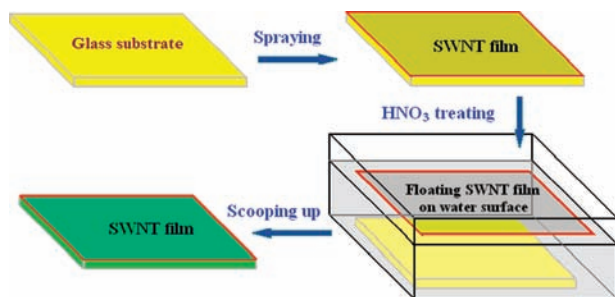


Figure 1. Fabrication, self-release, and transfer processes for thin SWNT films.

and then immersed in water. The SWNT films self-released from the substrate surface to form free-standing thin SWNT films on the water surface. The SWNT films floating on the water surface were transferred to a substrate such as a PET film. The fabrication, HNO_3 treatment, and transferring processes of the thin SWNT films are schematically shown in Figure 1.

Characterization. Raman measurements were carried out using a Renishaw Ramanscope (System 1000, excitation wavelength of 514 nm), laser Raman Spectrophotometers (Jobin Yvon LabRam HR800, excitation wavelength of 633 nm, and JASCO NRS-3100, excitation wavelength of 785 nm). Transparency measurements of the SWNT films were carried out using an UV–vis–near-IR spectrophotometer (JASCO V-570). The sheet resistances of the SWNT films deposited on glass and PET substrates were measured using a standard four-point probe configuration (Loresta-GP). A series of 5–6 measurements was taken on each film, and the measurements then were averaged to give the final reported value with the standard deviation as the error range. The surface topology of the thin SWNT films was examined using an AFM microscope (Shimadzu, SPM 9600) in the tapping mode in the air. The average surface roughness of the SWNT films was examined from AFM images with a size of $10 \times 10 \mu\text{m}^2$. In order to estimate the length of different SWNTs, a small drop of the dilute SWNT suspension was dropped and spin coated onto a clean mica substrate and the obtained SWNT film on the mica substrate was used for AFM observations.

Results and Discussion

In this study, we used the F-SWNTs that were synthesized in a quartz tube reactor inside an electrical furnace. When compared to the conventional floating catalyst CVD procedure,^{34,35} high H_2 flow, ultralow CH_4 flow, and a precise amount of catalyst precursor and growth promoter (sulfur) were utilized to stabilize the SWNT growth in order to realize a better control on the SWNT structure.^{25,33} Such ultralong, uniform, nearly defect-free, ultraclean F-SWNTs with high quality are very attractive materials for fabricating ultrathin SWNT films with high conductivity and transparency. In the spraying process, the SWNTs tended to lie parallel to the substrate surface, gained maximal overlap and interpenetration, and thus formed a uniform ultrathin network with a random in-plane orientation. Therefore, the spray-coated F-SWNT films are highly transparent as shown in Figure 2a probably due to their homogeneous thickness, which can be controlled with high precision by adjusting the sprayed volume of the SWNT solution. If a SWNT film is not very homogeneous, due to the severe diffusion of light, it will lose high transparency even if it is very thin.²⁴

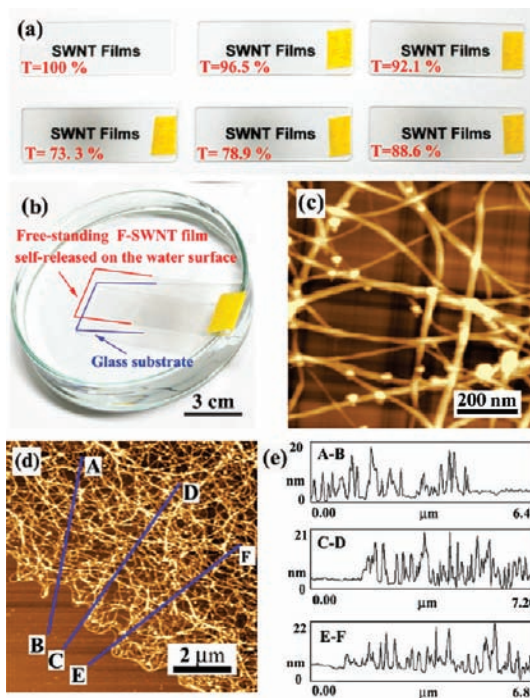


Figure 2. (a) Photograph of the spray-coated F-SWNT films on glass substrates ($26 \times 76 \text{ mm}^2$) before HNO_3 treatment with a different transmittance (T) at 550 nm placed on a paper with printed “SWNT Films” to illustrate the transparency; note that the top-left glass substrate has no SWNT-network coating for comparison. (b) Photograph of the HNO_3 -treated ultrathin F-SWNT film of ~ 20 -nm thickness self-released on the water surface. (c and d) Atomic force microscopy (AFM) images of the transferred F-SWNT film on mica. (e) Height profiles measured by line scans along A–B, C–D, and E–F directions in d.

We discovered that after the HNO_3 treatment, the F-SWNT films (i.e., even ~ 20 nm in thickness) resulted in a nondestructive self-release process from the glass substrates to form free-standing continuous thin films on the water surface while maintaining their original sizes. Figure 2b shows the self-release process on the water surface for the HNO_3 -treated F-SWNT film with an ~ 20 nm thickness supported on the glass substrate. This film shows an extremely high transmittance of $\sim 94\%$ at 550 nm on the PET or glass substrate only with a conductivity of $\sim 650 \Omega/\text{sq}$. In comparison, the vacuum-filtered ultrathin SWNT films are very notorious for their poor conductivities at high transmittance (i.e., over 90%) at a low SWNT loading,³¹ because these films obtained by vacuum filtration contain partially vertically aligned nanotubes that formed in the filter pores by the flow,²¹ which decreases the density of the nanotube network structures. Although Saran et al.⁹ successfully obtained high-quality laser-SWNT films with a very high conductivity of $\sim 80 \Omega/\text{sq}$ at an $\sim 80\%$ optical transparency on PET substrates without any post-treatments, their films are rather thick (~ 1500 nm).

In fact, all the as-prepared F-SWNT films with various thickness (i.e., ~ 20 – 140 nm) can provide free-standing films on the water surface (see Supporting Information, Figure S2). In stark contrast, without the HNO_3 -treatment process, the F-SWNT films were not released from the substrate surfaces, when immersed in water even for months. It is clear that the HNO_3 treatment sufficiently weakened the adhesion of the SWNTs to the substrate surfaces. It should be noted that special care should be taken for the choice of HNO_3 concentration, because low-concentration HNO_3 solution (i.e., < 4 M) did not effectively eliminate the adhesion of the films to the substrate

(34) Cheng, H. M.; Li, F.; Su, G.; Pan, H. Y.; He, L. L.; Sun, X.; Dresselhaus, M. S. *Appl. Phys. Lett.* **1998**, *72*, 3282.

(35) Cheng, H. M.; Li, F.; Sun, X.; Brown, S. D. M.; Pimenta, M. A.; Marucci, A.; Dresselhaus, G.; Dresselhaus, M. S. *Chem. Phys. Lett.* **1998**, *289*, 602.

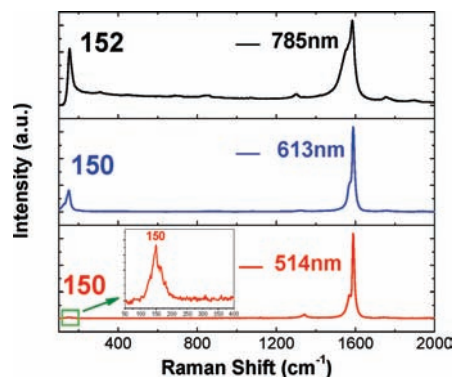


Figure 3. Raman spectra of the F-SWNTs excited by laser wavelength of 514, 613, and 785 nm.

surfaces, while high-concentration HNO_3 (i.e., >7 M) might seriously destroy the tube–tube junction and cause the films to fragment into smaller pieces (see Supporting Information, Figure S3).

Figure 2c shows the AFM image of the free-standing F-SWNT film transferred on a mica substrate, in which we see a loose mesh-like network structure. The hydrophobic nature together with the mechanical toughness of the F-SWNTs may contribute to the water floating of the films with such a network structure. It can be seen that the thickness of the film (Figure 2d) was ~ 20 nm and rather uniform from the height profile (Figure 2e). The average surface roughness of this SWNT film was about 3.3 nm within a given area of $10 \times 10 \mu\text{m}^2$, which is comparable to that of the ultrasmooth SWNT films³² but smaller than those of other SWNT films reported in the literature.^{31,36,37} In our experiments, the average surface roughness of the SWNT films slightly increased with an increase in the film thickness, whereas the average roughness of the SWNT films with a thickness of over 50 nm remained at about ~ 7 nm.

Four other different SWNT materials that included the A-, CM-, H-, and f-SWNTs were used for comparison. It was found that only the A- and f-SWNT films with thicknesses over 50 nm after the HNO_3 treatment can successfully be self-released from the deposited glass substrates, whereas the thinner films with a thickness of less than 50 nm were unable to form free-standing films on the water surface; in stark contrast, no CM- and H-SWNT films supported on the glass substrates could form free-standing films on the water surface, probably due to their poor mechanical property (see Supporting Information, Figure S4). Since all preparation procedures were almost the same, the difference in the formation of the free-standing films should originate from the different intrinsic properties of the starting SWNT materials. To clarify this point, the microstructures of these SWNTs were investigated and compared.

The structures of the A-, CM-, H-, and f-SWNTs were characterized by Raman analysis (see Supporting Information, Figure S5). Figure 3 shows the Raman spectra of the F-SWNTs with excitation laser wavelengths of 514, 613, and 785 nm. The very small D band and a small intensity ratio of D to G bands indicate the high purity of the nanotubes together with their high crystallinity. The single radial breathing mode (RBM) peak that is inversely proportional to the SWNT diameter demon-

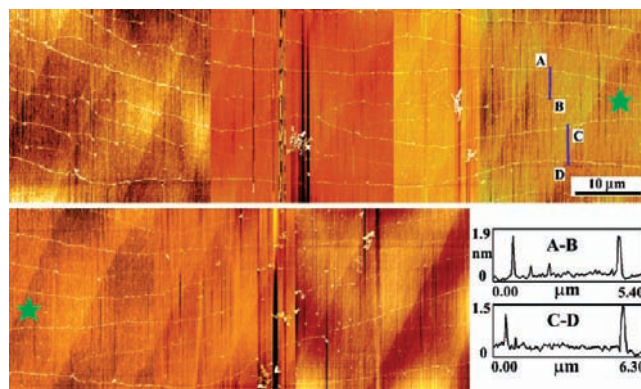


Figure 4. AFM image of the isolated F-SWNTs and height profiles measured by line scans along A–B and C–D directions. The two green pentacles in the AFM image indicate the same spot.

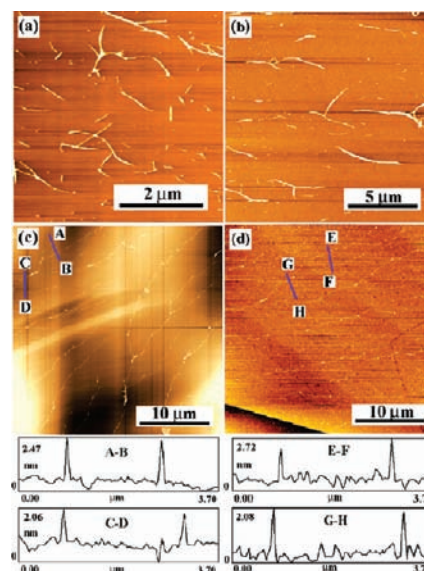


Figure 5. AFM images of (a) CM-, (b) H-, (c) A-, and (d) f-SWNTs, revealing different length distributions. Insets in c and d are the corresponding height profiles measured by line scans along A–B and C–D in c and E–F and G–H in d.

strates the exceptionally uniform large diameter (~ 1.6 nm) of the F-SWNTs, which favors formation of a uniform SWNT network structure with a very small surface roughness. Figure 4 shows the AFM image of the individually dissolved F-SWNTs that show an ultralong length. The height profiles (inset in Figure 4) demonstrate that the diameter of the tubes is ~ 1.5 – 1.8 nm, which agrees with the Raman data described above. We now can determine that the lengths of the F-SWNTs are over $100 \mu\text{m}$. The length-dependent mechanics of nanotube networks indicates that the ultralong length of nanotubes can increase the network formation with an ultrathin thickness with a very high degree of entanglement and therefore can greatly increase the mechanical properties of the resulting CNT films.³⁸

The lengths of the four other SWNTs, i.e., the A-, CM-, H-, and f-SWNTs, were also roughly estimated by AFM observations, as shown in Figure 5. It can be concluded that the nanotube length is as follows: F-SWNTs ($>100 \mu\text{m}$) $>$ f-SWNTs ($<100 \mu\text{m}$) \approx A-SWNTs ($<100 \mu\text{m}$) $>$ H-SWNTs (~ 3 – $10 \mu\text{m}$)

(36) Zhang, D. H.; Ryu, K.; Liu, X. L.; Polikarpov, E.; Ly, J.; Tompson, M. E.; Zhou, C. W. *Nano Lett.* **2006**, *6*, 1880.

(37) Geng, H. Z.; Kim, K. K.; So, K. P.; Lee, Y. S.; Chang, Y.; Lee, Y. H. *J. Am. Chem. Soc.* **2007**, *129*, 7758.

(38) Rahatekar, S. S.; Koziol, K. K.; Kline, S. R.; Hobbie, E. K.; Gilman, J. W.; Windle, A. H. *Adv. Mater.* **2009**, *21*, 874.

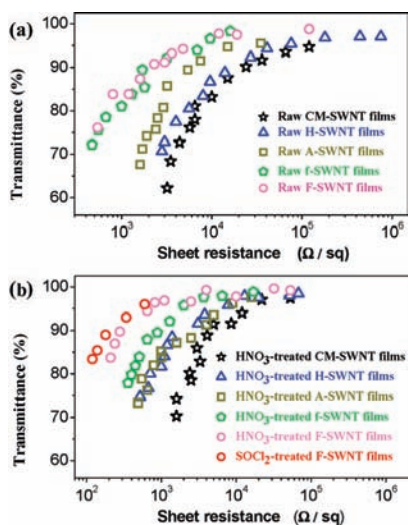


Figure 6. Plots of the sheet resistance vs transmittance for the spray-coated thin films of A-, CM-, H-, f-, and F-SWNTs (a) before and (b) after HNO_3 treatment.

> CM-SWNTs ($\sim 1\text{--}3\ \mu\text{m}$). In contrast to the ultralong F-SWNTs, the short CM- and H-SWNTs tended to form networks through aggregation rather than overlap. Therefore, the thin CM- and H-SWNT films severely lacked mechanical flexibility and thus were readily dispersed into smaller flakes by the shear stresses of solution during their self-release processing. In addition, the impurities, such as amorphous carbon attached to the outer surface of nanotubes, may also decrease the overlap degree of nanotubes. For example, AFM images reveal that the $\sim 50\ \text{nm}$ thick H-SWNT films have many large bundles and “bumps” protruding from the film surface (see Supporting Information, Figure S6), which resulted in a high average surface roughness of $\sim 14\ \text{nm}$ for a displayed $10 \times 10\ \mu\text{m}$.

It has been reported that the yield stress for the short nanotube network is an order of magnitude below that of the long nanotube network, even though the concentration of the shorter nanotubes is three times higher.³⁸ Therefore, almost all CM- and H-SWNT films failed to release from the glass substrates. In our experiments, the H-SWNT films even as thick as up to $\sim 150\text{--}250\ \text{nm}$ were unable to form free-standing films on the water surface (see Supporting Information, Figure S7). However, at the sufficient SWNT loading, long A- and f-SWNTs can form thin networks with mechanical flexibility through overlap. As a result, the A- and f-SWNT films over $50\ \text{nm}$ in thickness are self-released from the deposited substrates, whereas the A- and f-films with ultrathin thickness (i.e., less than $50\ \text{nm}$) failed to form free-standing films on the water surface. For the same reason, it can be understood why all the F-SWNT films with different thicknesses, which were fabricated from high-quality ultralong F-SWNTs, successfully form free-standing films on the water surface while maintaining their original sizes and network structures.

More importantly, different starting SWNT materials used to fabricate films also resulted in striking changes in the optical and electronic properties of these films. Figure 6 summarizes the transmittance vs sheet resistance of the films made from A-, CM-, H-, f-, and F-SWNTs. At identical transmittances, it can be seen that the conductivities of these films follow F-SWNTs \approx f-SWNTs > A-SWNTs > H-SWNTs > CM-SWNTs (Figure 6a), while after HNO_3 treatment they follow

F-SWNTs > f-SWNTs > A-SWNTs \approx H-SWNTs > CM-SWNTs (Figure 6b). HNO_3 treatment can remove the insulating SDS molecules from these SWNT films, enhance the SWNT network junctions, and improve the flexibility and conductivity of the SWNTs,³⁷ and therefore, the optical and electronic properties of these SWNT films are sharply improved after HNO_3 treatment. For instance, an F-SWNT film with a sheet resistance of $\sim 540\ \Omega/\text{sq}$ at an $\sim 76\%$ optical transparency reached $210\ \Omega/\text{sq}$ at an $\sim 84\%$ optical transparency after HNO_3 treatment. In addition, after doping with SOCl_2 ,³⁹ the conductivity of this film could be further improved to $120\ \Omega/\text{sq}$ at an $\sim 83\%$ optical transparency, which is close to that of conventional indium–tin oxide (ITO). It should be noted that although only water washing can remove part of the superfluous SDS in the SWNT networks, the change in the conductivity of the SWNT films is almost negligible (see Supporting Information, Figure S8).

Compared to the A-, CM-, H-, and f-SWNT films, the F-SWNT films consistently exhibited the highest conductivities at identical optical transmittances. We believe that the overall excellent structural properties of the F-SWNTs, such as long length, uniform diameter, and a low defect ratio, which have been demonstrated by Raman analysis and AFM observations, collectively made such a remarkable difference. The ultralong length, high purity, and high crystallinity of nanotubes substantially decrease the resistivity of SWNT–SWNT junctions in the F-SWNT networks. The exceptionally uniform large diameter of the F-SWNTs not only favors formation of uniform networks with a very small surface roughness but also minimizes the band gap of the SWNTs and therefore are much preferable for conductive and transparent thin films.⁴⁰ As a result, the F-SWNT films are reasonably expected with more excellent optical and electronic properties than those of the A-, CM-, H-, and f-SWNT films.

In stark contrast to the ultralong F-SWNTs, the shortest CM-SWNTs significantly increase the resistivity of the SWNT–SWNT junctions in the nanotube networks, so the CM-SWNT films exhibit a very poor conductivity. Due to the defect-healing effect induced by superhigh plasma temperature in the arc growth process,²⁷ the A-SWNTs have higher structural integrity than that of the CM- and H-SWNTs synthesized at moderate CVD temperature, which is reflected by their smaller intensity ratio of the D to G bands in the Raman spectra. Therefore, the conductivities of the A-SWNT films are reasonably higher than those of the CM- and H-SWNT films at identical optical transmittances. On the other hand, the arc-discharged method is notorious for producing SWNTs combined with many nontubular impurities such as graphitic layers and amorphous carbon. That may be the reason for the conductivities of the A-SWNT films being lower than those of the f-SWNT films at identical optical transmittances, although their length distributions are not very different. However, for the regions of over 98% transparency, the sheet resistances of the SWNT films sharply increase with their transparency, which makes all the curves of the transmittance vs sheet resistance of the five types of SWNTs trend to merge together whether or not the SWNT films are post-treated. Such aspects are mainly due to the discontinuity among the SWNTs in the films, regardless of the type of the SWNTs.

(39) Li, Z.; Kandel, H. R.; Dervishi, E.; Saini, V.; Xu, Y.; Biris, A. R.; Lupu, D.; Salamo, G. J.; Biris, A. S. *Langmuir* **2008**, *24*, 2655.

(40) Cao, Q.; Rogers, J. A. *Adv. Mater.* **2009**, *21*, 29.

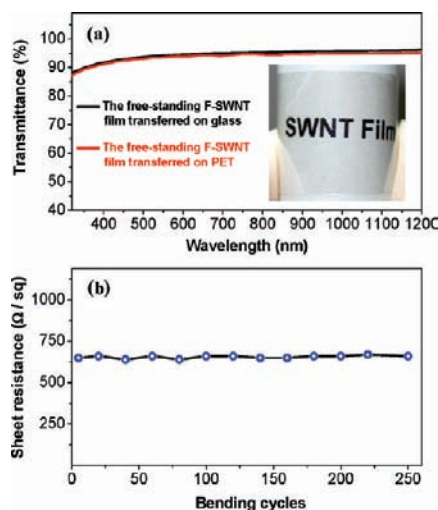


Figure 7. (a) Transmittance spectra of the ~ 20 nm thick F-SWNT film on glass substrate (black) and transferred to a PET substrate (red); (inset) photograph of this film on the PET over a 2 cm diameter cylinder. (b) Plots of sheet resistance of this film on the PET as a function of bending cycles.

The free-standing F-SWNT films can be easily and safely transferred to any substrate of interest. For instance, an ~ 20 nm thick F-SWNT film transferred on a flexible PET substrate exhibits high transparency ($>90\%$) over a broad spectral range (Figure 7a), retaining its original optical feature. The transferred F-SWNT film can be bent into a 2 mm radius over 200 times without a change in sheet resistance of $\sim 650 \Omega / \text{sq}$ (Figure 7b). The mesh-like structure framed by random orientation of the F-SWNTs may absorb the morphological variation to retain the original performance. Moreover, the transferred F-SWNT film had a strong adhesion to the PET surface, which resembles a previously reported behavior.⁹ In our experiments, after soaking in water over months or sonication for tens of minutes, the transferred F-SWNT films were not fragmented or peeled off the PET substrates. Such aspects make the F-SWNT films

promising as functional materials for a variety of rolled-up electronic/optical devices against tearing or damage.

Conclusions

In summary, we demonstrated a simple and robust approach to the preparation of free-standing ultrathin F-SWNT films with high transmittance and conductivity. The optical, electronic, and self-release properties of the SWNT films strongly depend on the starting SWNTs used to fabricate thin films. The utilization of high-quality F-SWNTs combined with appropriate HNO_3 treatment plays a significant role in the self-release process of the F-SWNT films. The obtained free-standing ultrathin F-SWNT films are mechanically flexible, which has a great advantage over conventional ITO and, therefore, strongly promise to be “post ITO”. By comparison to the conventional four different SWNTs, we revealed that high-quality ultralong F-SWNTs (over $100 \mu\text{m}$) play an important role in the formation of free-standing ultrathin (~ 20 nm) films that can be transferred to flexible transparent films, which will expand their fundamental research and novel applications.

Acknowledgment. The authors acknowledge financial support from the Global COE Program “Science for Future Molecular Systems” (Kyushu University) from the Ministry of Education, Culture, Sports, Science and Technology, Japan. H.M.C. acknowledges support from NSFC (No. 50921004).

Supporting Information Available: Photographs of the spray-coated F-SWNT films with different thickness and their self-release from glass substrates on water surface, photographs of A-, CM-, H-, and f-SWNT films self-released from glass substrates on water surface, Raman spectra and AFM images of A-, CM-, H-, and f-SWNTs, plots of the sheet resistance vs transmittance for the F-SWNT films without any post treatment and with water and HNO_3 treatment. This material is available free of charge via the Internet at <http://pubs.acs.org>.

JA1067367